Aveolar Macrophage Activation and Cytokine Storm in the Pathogenesis of Severe COVID-19

Chaofu Wang (wangchaofu@126.com)
Department of Pathology, Ruijin Hospital, Shanghai Jiaotong University School of Medicine

Jing Xie
Department of Pathology, Ruijin Hospital, Shanghai Jiaotong University School of Medicine

Lei Zhao
Department of Pathology, Shanghai Jiaotong University School of Medicine

Xiaochun Fei
Department of Pathology, Ruijin Hospital, Shanghai Jiaotong University School of Medicine

Heng Zhang
Department of Pathology, Ruijin Hospital, Shanghai Jiaotong University School of Medicine

Yun Tan
National Research Center for Translational Research (Shanghai), Ruijin Hospital, Shanghai Jiaotong University School of Medicine

Luting Zhou
Department of Pathology, Ruijin Hospital, Shanghai Jiaotong University School of Medicine

Zhenhua Liu
Department of Ultra-sound, Ruijin Hospital, Shanghai Jiaotong University School of Medicine

Yong Ren
General Hospital of Central Theater Command, PLA

Ling Yuan
General Hospital of Central Theater Command, PLA

Yu Zhang
General Hospital of Central Theater Command, PLA

Jinsheng Zhang
General Hospital of Central Theater Command, PLA

Liwei Liang
General Hospital of Central Theater Command, PLA

Xinwei Chen
General Hospital of Central Theater Command, PLA

Xin Liu
General Hospital of Central Theater Command, PLA

Peng Wang
General Hospital of Central Theater Command, PLA

Xiao Han
General Hospital of Central Theater Command, PLA
Xiangqin Weng
National Research Center for Translational Research (Shanghai), Ruijin Hospital, Shanghai Jiaotong University School of Medicine
Ying Chen
Wuhan Institute of Virology, Chinese Academy of Sciences
Ting Yu
Department of Pathology, Jin Yin-tan Hospital
Xinxin Zhang
Research Laboratory of Clinical Virology, Ruijin Hospital and Ruijin Hospital North, Shanghai Jiaotong University School of Medicine
Jun Cai (caijun@shsmu.edu.cn)
Department of Pathology, Shanghai Jiaotong University School of Medicine
Rong Chen (crjudy@126.com)
Department of Pathology, Jin Yin-tan Hospital
Zhengli Shi (zlshi@wh.iov.cn)
Wuhan Institute of Virology, Chinese Academy of Sciences
Xiuwu Bian (bianxiuwu@263.net)
Institute of Pathology and Southwest Cancer Center, Southwest Hospital, Third Military Medical University (Army Medical University), Key Laboratory of the Ministry of Education

Research Article

Keywords: COVID-19, pathogenesis, fatal cases, gross anatomy, molecular markers

Posted Date: March 26th, 2020

DOI: https://doi.org/10.21203/rs.3.rs-19346/v1

Abstract

The coronavirus disease-19 (COVID-19) caused by SARS-CoV-2 infection can lead to a series of clinical settings from non-symptomatic viral carriers/spreaders to severe illness characterized by acute respiratory distress syndrome (ARDS)1,2. A sizable part of patients with COVID-19 have mild clinical symptoms at the early stage of infection, but the disease progression may become quite rapid in the later stage with ARDS as the common manifestation and followed by critical multiple organ failure, causing a high mortality rate of 7-10% in the elderly population with underlying chronic disease1-3. The pathological investigation in the lungs and other organs of fatal cases is fundamental for the mechanistic understanding of severe COVID-19 and the development of specific therapy in these cases. Gross anatomy and molecular markers allowed us to identify, in two fatal patients subject to necropsy, the main pathological features such as exudation and hemorrhage, epithelium injuries, infiltration of macrophages and fibrosis in the lungs. The mucous plug with fibrinous exudate in the alveoli and the activation of alveolar macrophages were characteristic abnormalities. These findings shed new insights into the pathogenesis of COVID-19 and justify the use of interleukin 6 (IL6) receptor antagonists and convalescent plasma with neutralizing antibodies against SARS-CoV-2 for severe patients.

Authors Chaofu Wang, Jing Xie, Lei Zhao, Xiaochun Fei, Heng Zhang, and Yun Tan contributed equally to this work.

Authors Chaofu Wang, Jun Cai, Rong Chen, Zhengli Shi, and Xiuwu Bian jointly supervised this work.

Introduction

Introduction section not provided with this version.

Results And Discussion

The two body donors of fatal cases with COVID–19 were a 53 years old female and a 62 years old male, respectively. Both patients had progressively decreased lymphocytes with elevated serum IL–6 and C reactive protein (CRP) levels in the late stage of disease (Supplementary Table 1), which was consistent with recent report1,2. The gross anatomy of the lung showed moderate bilateral pleural effusion and pleural adhesion in the two patients. The hepatization of lung tissues was observed on the cut-surface of the collapsed and consolidated lungs. The microscopic manifestation of the lung injury was consistent with diffuse alveolar damage (DAD). Alveolar cavities were filled with a large number of macrophages with scattered neutrophils and lymphocytes (Fig. 1a). The massive serous (Fig. 1b) and fibrinoid exudate in the alveolar spaces were shown by the Masson staining (Fig. 1c, d). The acidic mucopolysaccharides from a large amount of mucinous secretion were observed by the Alcian blue-periodic acid-Schiff (AB-PAS) staining in the bronchi and bronchioles, terminal bronchioles and pulmonary alveoli (Fig. 1e, f). A lot of mucus in the distal respiratory tract lined by mucous cells were shown, reminiscent of the morphology of mucoid adenocarcinoma (Fig. 1g). The peribronchiolar metaplasia (PBM) with interstitial fibrous

hyperplasia but without invasive growth of atypical cells was observed. The mucous plug with fibrinous exudate in the alveoli and terminal bronchioles formed the cribriform pattern. The bronchial phlegm combined with epithelial detachment and fibrinoid exudate was visible (Fig. 1h).

The hyaline membranes and widened alveolar walls with collagen fibers proliferation and lymphocyte infiltration were observed in alveoli occasionally (Extended Data Fig. 1a, b). Focal or patchy hemorrhage with fibrinous exudate were seen in the alveolar cavities and interstitial tissues (Extended Data Fig. 1c, d). The broken alveolar walls flushed by huge hemorrhagic effusion formed the “blood lake”. The endothelial cells of small pulmonary arteries were swollen and shed (Extended Data Fig. 1e). Mixed thrombi were present in small veins (Extended Data Fig. 1f).

Intensive loss of bronchiole and alveolar epithelial cells was remarkable (Fig. 2a, b) while abundant swollen and degenerated alveolar cells desquamated in the alveoli (Fig. 2c, d). Patchy type II pneumocytes proliferated with atypical changes, including enlarged nuclei, clearing of nuclear chromatin, prominent nucleoli and suspected viral inclusions (Fig. 2e, f). The notable proliferation of type □ alveolar epithelial cells resembled the morphological changes of atypical adenomatous hyperplasia, in situ adenocarcinomas, or even invasive adenocarcinoma. Thickened alveolar walls and widened interstitial tissues were accompanied by lymphocyte infiltration and fibroblast proliferation (Fig. 2g, h).

Notably, the alveolar macrophages significantly increased and filled in a part of the alveolar cavities with scattered neutrophils and lymphocytes. CD68, one of the scavenger receptors, is a well-documented specific surface marker of macrophages4. The alveolar macrophages were presented in diverse forms, including aggregation in small clusters (Fig. 3a, b), diffused distribution (Fig. 3c), single macrophage exhibiting intracytoplasmic phagocytosis, spherical acidophilic hyaline bodies or hemophagocytic phenomenon (Fig. 3d, e), and multinucleated giant cells (Fig. 3f). Furthermore, using immunohistochemistry approach, we examined several chemokine and inflammatory cytokines secreted by alveolar macrophages including IL−6, IL-10 and TNFα with specific antibodies. IL−6 and TNFα were moderately expressed in macrophages (Fig. 3g, i), while the expression of IL−10 was strong (Fig. 3h). Besides, extensive and strong expression of Programmed Death-Ligand 1 (PD-L1) was observed (Fig. 3j).

In general, the degree of infiltration of lymphocytes into the pulmonary tissues was much inferior to that of macrophages, although some focal lymphocyte infiltrations were present in lungs (Extended Data Fig.2a). CD20-positive B lymphocytes (Extended Data Fig.2b) accounted for a large majority of the lymphocytes whereas a few CD3-positive T lymphocytes (Extended Data Fig.2c) made up a small proportion including CD4-strong positive for helper T cells (Extended Data Fig.2d) and CD8-positive for cytotoxic T cells (Extended Data Fig.2e). Among the inflammatory infiltrating cells, no CD56-positive NK/T cells (Extended Data Fig.2f) were detected. Neither Programed cell death protein−1 (PD−1) nor PD-L1 proteins were shown on the surface of lymphocytes (Extended Data Fig.2g, h). None of the lymphocytes were proven virus-infected by using immunohistochemistry of Rp3-NP specific antibodies (Extended Data Fig.2i).

We carefully examined the heart and kidney in the two donor bodies. No obvious gross abnormalities were observed. Nevertheless, microscopical abnormalities were observable in both organs. Multifocal myocardial degeneration was present in the heart, together with myocardial atrophy and interstitial fibrous tissue hyperplasia (Extended Data Fig.3a). A few CD20-positive B cells and CD3-positive T cells were scattered (Extended Data Fig. 3b, c). In the kidneys, normal renal structures were retained. However, the fibrotic glomeruli and edematous tubular epitheliums (Extended Data Fig.3d) were focally present with a small amount of infiltrating B (Extended Data Fig.3e) and T lymphocytes (Extended Data Fig.3f). It is worth noting that no viral particles were found in parenchymal cells in both heart and kidney.

Next, we examined lymph nodes and other lymphoid organs. Notably, lymph nodes in the pulmonary hilum were swollen whereas splenic volume was slightly reduced with shrunken capsule in the two cases. Morphological changes of the pulmonary hilum lymph nodes were characterized by an obvious dilation of cortical sinuses with numerous macrophages (Extended Data Fig.4e). In the spleen, the lymphocytes in the white pulp were slightly reduced with infiltration of macrophages in the red pulp (Extended Data Fig.4g). Notably, the hyperplastic type II alveolar epithelial cells, alveolar macrophages, macrophages in the pulmonary hilum lymph nodes and spleen were all infected by SARS-CoV–2 whereas no obvious viral infection was found in lymphocytes and mesenchymal cells (Extended Data Fig.4a-h).

An important finding in the present work was the infections of gastrointestinal mucosa cells (Extended Data Fig.4i) and spermatogenic testicular cells (Extended Data Fig.4k) by SARS-CoV–2 without obvious histological abnormalities. In addition, the intestinal epithelium cells, submucosa ganglion cells, spermatogenic Sertoli and Leydig cells were all infected by SARS-CoV–2 (Extended Data Fig.4j, l). Scrutiny of pathological sections of esophagus, breasts, muscles, stomach, thyroid, bladder and adrenal glands showed no obvious abnormalities or SARS-CoV–2 infection.

The pathological investigations of severe patients are pivotal for the understanding of pathogenesis of COVID–19 and assessment of clinical treatments. Lungs are the main damaged organ in severe COVID–19 patients due to the ARDS, similar to the situation in SARS outbreak of 2003. In this regard, the common features of lung injuries constituting the main pathological abnormalities somehow mimicked those in SARS, including: (1) extensive impairment of type I alveolar epithelial cells and atypical hyperplasia of type II alveolar cells; (2) formation of hyaline membrane, focal hemorrhage, exudation and pulmonary edema; (3) pulmonary consolidation with infiltration of macrophages, lymphocytes as well plasma cells; (4) endothelial injury and thrombosis in small vessels and microvascular. Thus, like SARS-CoV, SARS-CoV–2 was capable of triggering the pathogenesis and resulting in severe dysfunction of ventilation and gas exchange obstruction in patients5–9.

However, the pathology of lungs with SARS-CoV–2 infection also exhibited some distinct features as compared to that found in SARS patients. The hyaline membranes in alveoli, which constituted major anatomical abnormalities leading to gas exchange obstruction in SARS, were uncommon in COVID–19. On the other hand, we observed mucous plugs in all respiratory tracts, terminal bronchioles and pulmonary alveoli in COVID–19, and this was neither described in SARS5,7–11 nor in the recently

reported autopsy studies on COVID–19 patients12,13. Another unique feature of COVID–19 was the excessive mucus secretion with serous and fibrinous exudation, which could aggravate the dysfunction of ventilation. These findings suggested the existence of different pathogenic mechanisms responsible for the hypoxemia between COVID–19 and SARS patients. We found the hyperplasia and peribronchiolar metaplasia of mucosal epithelium, a phenomenon which might result from the inflammation- induced pulmonary tissue reparatory processes or even proliferative reaction of cells originated from bronchioles and terminal bronchioles. We assume that the mucus aggregation in distal respiratory tracts by peribronchiolar metaplasia of mucosal epithelium as a result of inflammation-induced reparatory changes should play a part in the sputum suction failure in very severe COVID–19 patients as previously reported12.

Of particular note, we found the alveolar macrophages with SARS-CoV–2 infection were expressing ACE2, a well-established receptor for both SARS-CoV and SARS-CoV–2 (Extended Data Fig.5). It was reported that SARS-CoV could occasionally be identified in the alveolar macrophages9. In COVID–19 patients, the extraordinary aggregation and activation of these macrophages could occupy a central position in pathogenesis of the very severe “inflammatory factor storm” or “cytokine storm”. Therefore, the spectacular infiltration and activation of alveolar macrophages in COVID–19, especially among patients with severe and critical stages of ARDS, might represent the shift of classically activated phenotype (M1) to alternatively activated phenotype (M2) of alveolar macrophages, whereas this shifted property of alveolar macrophages could contribute to the inflammatory injuries and fibrosis of respiratory tracts14. To further address the issue of accumulation of macrophages in lung tissues and to explore the potential function of macrophages in response to SARS-CoV–2, we incubated purified and Fc-tagged spike proteins (S protein), which contains the receptor binding domain (RBD) responsible for the entry of SARS-CoV–2 into the host cells15, with white blood cell samples from six healthy donors. The possible location of the S protein on the surface of these white blood cells was examined by flow cytometry analysis. To our surprise, the S protein interacted with CD68-expression monocytes/macrophages but not with T or B lymphocytes, suggesting a direct viral infection of the macrophage/monocytes. We then determined the expression of ACE2 on the surface of macrophages. Indeed, an expression pattern similar to the binding of S protein by monocytes/macrophages was observed (Fig. 4b). These findings highlighted the role of macrophages as direct host cells of SARS-CoV–2 and potential drivers of “cytokine storm syndrome” in COVID–19.

Additionally, an elevated serum IL–6 was observed in the two cases in this study and also in some other very recent reports16. These features were similar to the pathogenesis of “cytokine storm syndrome” in patients with hemophagocytic lymphohistocytosis (HLH) or macrophage activation syndrome (MAS)17,18. The blockage of cytokine storm using anti-IL–6 or IL–6R antibody, such as Tocilizumab, has promising therapeutic effects and clinical practice in the treatment of MAS or HLH. Therefore, our data are in support of the beneficial use of anti-IL- 6/IL–6R antibody for the inhibition of alveolar macrophage activation as well as inflammatory injuries in COVID–19 patients. Recently, the Tocilizumab therapy has been recommended in the Guideline of Diagnosis and Treatment of COVID–19 (version 7) by the National Health Commission.

The fact that the known ACE2-exressing cells19–21, including type II alveolar epithelial cells, alveolar macrophages, intestinal epithelial cells and spermatogenic cells, were all found infected by SARS-CoV–2 infection suggests the necessarily of clinical tests of SARS-CoV–2 in feces samples and the blockade of possible fecal-oral transmission22. Infected submucosa ganglion cells in small intestine were never reported before. Whether it could be the host cells for long-term coexistence of virus or not remains to be investigated. It is worth noting that remarkable viral infection persisted even at the end stage of COVID–19, when the viremia was well passed in the great majority of patients. Under this circumstance, use of specific anti-viral therapy should be encouraged. Recently, our group identified the convalescent plasma (CP) from recovered COVID–19 to be a specific and effective therapy for this disease, especially in severe cases, since the overwhelming majority of patients presented high neutralizing antibody titers against SARS-CoV–2 and the preliminary results of a phase I trial of CP showed very promising effects (Duan K, ZHANG XX, YANG XM et al, submitted).

Still, some issues remain to be addressed in future studies: first, what are the molecular and cellular mechanism underlying the infection of alveolar macrophages of SARS-CoV–2 should be illustrated so that a deeper understanding of the pathogenic role of viral infection and the mechanism for its escape from immune reaction can be achieved. These studies may accelerate smart drug and vaccine design targeting vulnerabilities of viral proliferation; Second, in the two cases studied here and in some other recent reports, there is a remarkable reduction of both CD4 and CD8 cells in the peripheral blood in COVID–19 patients. A graded decrease of T cells was found with increase clinical severity of COVID–19. Intriguingly, there is a negative correlation between the extent of T lymphocytopenia and increased IL–6 and Il–8 levels in the serum. The causal relationship between these two phenomena should be addressed; Third, in this study, no ACE2-expression was found on the surface of T cells, which may eliminate the possibility of a direct toxic effect of SARS-CoV–2 on distinct subsets of T cell population. However, only a small number of T lymphocytes were observed in the inflammatory lung tissues. This situation seems to be a paradox to the initial assumption that the severe T cell reduction could be ascribed to a tremendous infiltration of T cells into damaged lung tissues in response to the effect of IL–6 and other cytokines. The detailed mechanism of T cell depletion in severe COVID–19 certainly requires in-depth study in the future either among patients or in experimental animal models.

Declarations

Acknowledgements

We thank the support of the Shanghai Guangci Translational Medical Research Development Foundation. We thank Prof. Zhu Chen and Prof. Saijuan Chen from National Research Center for Translational Research (Shanghai), State Key Laboratory of Medical Genomics, Shanghai Institute of Hematology, Ruijin Hospital, Shanghai Jiaotong University School of Medicine and Prof. Guang Ning and Prof. Yanan Cao from National Clinical Research Centre for Metabolic Diseases, Shanghai Clinical Center for Endocrine and Metabolic Diseases, Ruijin Hospital, Shanghai Jiaotong University School of Medicine for

discussion and revision of the manuscript. The authors express highest respect to the two donor patients and their families for their great and generous support to the research on the pathogenesis of COVID–19.

Author contributions

C. W., J. X. and R. C. conceived and designed the study, L. Z., X. F., H. Z., Y. T., X. W., Z. L., Y. R., L. Y., Y. Z., J. Z., L. L., X. C., X. L., P. W., X. H., Y. C., T. Y. Z. S., performed experiments and data analysis. J. C., X. Z. and X. B. contributed to discussion and revision of the manuscript.

Competing interests

The authors declare no competing interests.

References

1. Huang, C. *et al.* Clinical features of patients infected with 2019 novel coronavirus in Wuhan, China. *Lancet* **395**, 497-506, doi:10.1016/S0140-6736(20)30183-5 (2020).
2. Guan, W. J. *et al.* Clinical Characteristics of Coronavirus Disease 2019 in China. *N Engl J Med*, doi:10.1056/NEJMoa2002032 (2020).
3. Chen, N. *et al.* Epidemiological and clinical characteristics of 99 cases of 2019 novel coronavirus pneumonia in Wuhan, China: a descriptive study. *Lancet* **395**, 507-513, doi:10.1016/S0140-6736(20)30211-7 (2020).
4. Kunisch, E. *et al.* Macrophage specificity of three anti-CD68 monoclonal antibodies (KP1, EBM11, and PGM1) widely used for immunohistochemistry and flow *Ann Rheum Dis* **63**, 774-784, doi:10.1136/ard.2003.013029 (2004).
5. Peiris, J. S. *et al.* Clinical progression and viral load in a community outbreak of coronavirus-associated SARS pneumonia: a prospective *Lancet* **361**, 1767-1772, doi:10.1016/s0140-6736(03)13412-5 (2003).
6. Ksiazek, T. G. *et al.* A novel coronavirus associated with severe acute respiratory syndrome. *N Engl J Med* **348**, 1953-1966, doi:10.1056/NEJMoa030781 (2003).
7. van der Hoek, L. *et al.* Identification of a new human coronavirus. *Nat Med* **10**, 368- 373, doi:10.1038/nm1024 (2004).
8. Ding, Y. *et al.* The clinical pathology of severe acute respiratory syndrome (SARS): a report from China. *J Pathol* **200**, 282-289, doi:10.1002/path.1440 (2003).
9. Nicholls, M. *et al.* Lung pathology of fatal severe acute respiratory syndrome. *Lancet***361**, 1773-1778, doi:10.1016/s0140-6736(03)13413-7 (2003).
10. Lee, *et al.* A major outbreak of severe acute respiratory syndrome in Hong Kong. *N Engl J Med* **348**, 1986-1994, doi:10.1056/NEJMoa030685 (2003).

11. Drosten, C. *et al.* Identification of a novel coronavirus in patients with severe acute respiratory syndrome. *N Engl J Med* **348**, 1967-1976, doi:10.1056/NEJMoa030747 (2003).
12. Xu, Z. *et al.* Pathological findings of COVID-19 associated with acute respiratory distress syndrome. *Lancet Respir Med*, doi:10.1016/S2213-2600(20)30076-X (2020).
13. Tian, *et al.* Pulmonary Pathology of Early-Phase 2019 Novel Coronavirus (COVID-19) Pneumonia in Two Patients With Lung Cancer. *J Thorac Oncol*, doi:10.1016/j.jtho.2020.02.010 (2020).
14. Hussell, & Bell, T. J. Alveolar macrophages: plasticity in a tissue-specific context.*Nat Rev Immunol* **14**, 81-93, doi:10.1038/nri3600 (2014).
15. Zhou, P. *et al.* A pneumonia outbreak associated with a new coronavirus of probable bat origin. *Nature* **579**, 270-273, doi:10.1038/s41586-020-2012-7 (2020).
16. Zhou, F. *et al.* Clinical course and risk factors for mortality of adult inpatients with COVID-19 in Wuhan, China: a retrospective cohort *Lancet*, doi:10.1016/S0140- 6736(20)30566-3 (2020).
17. Billiau, A. D., Roskams, T., Van Damme-Lombaerts, R., Matthys, P. & Wouters, C. Macrophage activation syndrome: characteristic findings on liver biopsy illustrating the key role of activated, IFN-gamma-producing lymphocytes and IL-6- and TNF-alpha- producing macrophages. *Blood* **105**, 1648-1651, doi:10.1182/blood-2004-08-2997 (2005).
18. Cheung, C. Y. *et al.* Cytokine responses in severe acute respiratory syndrome coronavirus-infected macrophages in vitro: possible relevance to pathogenesis. *J Virol* **79**, 7819-7826, doi:10.1128/JVI.79.12.7819-7826.2005 (2005).
19. Wang, Z. & Xu, X. scRNA-seq Profiling of Human Testes Reveals the Presence of ACE2 Receptor, a Target for SARS-CoV-2 Infection, in Spermatogonia, Leydig and Sertoli Cells. *Preprints*, doi:10.20944/preprints202002.0299.v1 (2020).
20. Zhao, Y. *et al.* Single-cell RNA expression profiling of ACE2, the putative receptor of Wuhan 2019-nCov. *bioRxiv*, doi:doi.org/10.1101/2020.01.26.919985 (2020).
21. Zou, X. *et al.* Single-cell RNA-seq data analysis on the receptor ACE2 expression reveals the potential risk of different human organs vulnerable to 2019-nCoV *Front Med*, doi:10.1007/s11684-020-0754-0 (2020).
22. Ling, *et al.* Persistence and clearance of viral RNA in 2019 novel coronavirus disease rehabilitation patients. *Chin Med J (Engl)*, doi:10.1097/CM9.0000000000000774 (2020).

Methods

Patients and pathological anatomy

The autopsy and pathological investigations of specimens were performed on body donors of two fatal cases with COVID−19 in Wuhan Jin Yin-Tan Hospital, Hubei, China. The diagnosis was established according to clinical symptoms (fever and cough), RT-PCR testing of SARS- CoV−2 and computed tomographic (CT) scanning examination. The severe hypoxemia caused by respiratory failure and circulatory failure was considered the critical cause of death in the two patients. Informed consent was

obtained. This study was approved by the Medical Ethics Committee of the National Health Commission of China. The autopsy procedures were performed in the negative pressure-ventilation P3 Laboratory.

Histological, histochemical and immunohistochemical staining

Hematoxylin and eosin (HE) staining of the slides of 10% neutral formaldehyde-fixed, paraffin-embedded tissues was performed and carefully reviewed on each patient. Alcian blue/periodic acid-Schiff (AB-PAS) staining and Masson staining were carried out for the examinations of mucus, fibrin and collagen fiber in lung tissues. Immunohistochemical staining was performed on the slides of lung tissues from two patients. A panel of primary antibodies were used, including the macrophage marker CD68 (Monoclonal mouse anti-human CD68, clone KP1; 1:100; Dako Omnis, Agilent); T-lymphocyte marker CD3 (Monoclonal rabbit anti-human CD3, clone SP7; ready-to-use; Dako Omnis, Agilent), CD4 (Monoclonal mouse anti-human CD4, clone 4B12; ready-to-use; Dako Omnis, Agilent) and CD8 (Monoclonal mouse anti-human CD8, clone C8/144B; ready-to-use); B-lymphocyte markers CD20 (Monoclonal mouse anti-human CD20cy, clone L26; ready-to-use); natural killer cell/T cell (NK/T cell) marker CD56 (Monoclonal mouse anti-human CD56, clone 123C3; ready-to- use), and the markers of Programmed Cell Death–1 (PD–1 Monoclonal mouse anti-human PD- 1, clone UMAB199; ready-to-use) and Programmed Cell Death-Ligand 1 (PD-L1 Monoclonal mouse anti-human PD-L1, clone 22C3; ready-to-use). Antibodies specific for chemokine and inflammatory cytokines were also used, including interleukin 6 (polyclonal rabbit anti-IL–6 human; 1:250; abcam), interleukin 10 (IL–10polyclonal rabbit anti-human IL–10; 1:300; abcam) and tumor necrosis factor α (TNFα, polyclonal rabbit anti-human TNFα; 1:80; abcam). In addition, ACE2 protein was revealed using a mouse monoclonal anti-human ACE2 antibody (clone 1G4; 1:160; ORIGENE) while the detection of /SARS-CoV–2 was performed using the antibody against SL-CoV Rp3 N-protein (Rp3-NP) (1:100; the Rp3-NP antibody was provided by Prof. Zheng-Li Shi, Wuhan Institute of Virology, Chinese Academy of Sciences).

Flow cytometry analysis

The white blood cells were obtained from six health donors according to manufactures' instructions of Red Blood Cell Lysis Buffer (#40401ES60, Yeasen, China). After the removal of the red blood cells, white blood cells were washed twice with PBS. Cells were firstly incubated with SARS-CoV–2 (2019-nCoV) Spike Protein (S1 Subunit, Fc Tag) (#40591-V02H, Sino Biological, China) or antibodies against human ACE2 (#21115–1-AP, Proteintech, China) in DMEM (Gibico) supplemented with 10% FBS (Gibico) for 30 minutes at room temperature. The cells were washed and used for flow cytometry labeling. Antibodies against human CD3 (APC mouse anti-human CD3 monoclonal antibody, clone HIT3a, BD Bioscience), CD14 (FITC mouse anti-human CD14 monoclonal antibody, clone RMO52, Beckman Coulter), CD68 (PE/Cy7 mouse anti-human CD68 monoclonal antibody, clone Y1/82A, Biolegend) and human IgG (PE anti-human IgG Fc, clone M1310G05, Biolegend) were used as primary antibodies and rabbit IgG (Alexa Fluor 546 Goat anti-Rabbit IgG (H+L) polyclonal antibody, ThermoFisher) were used as secondary

antibodies, according to manufactures' instructions. BD LSRFortessa™ X–20 was used for flow cytometry analysis.

Figures

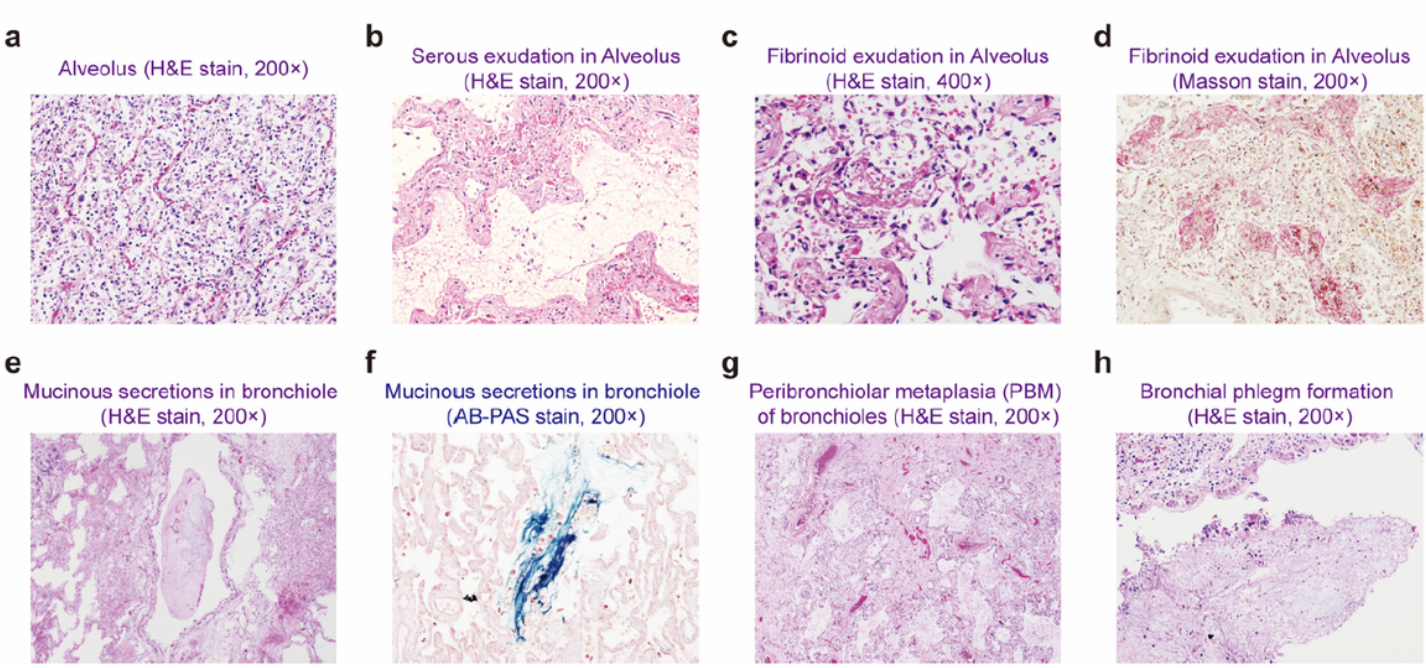

Figure 1

Extensive exudate and mucinous secretion. a, A large number of macrophages in alveolar cavities (H&E stain, 200×). b-d, Serous (b, H&E stain, 200×) and fibrinoid (c, H&E stain, 400×, d, Masson stain, 200×) exudation. e-h, Mucinous secretions in bronchioles (e, H&E stain, 100×) with blue staining by AB-PAS (f, H&E stain, 200×). Abnormalities mimicking peribronchiolar metaplasia (PBM) of bronchioles and terminal bronchioles (g, H&E stain, 100×) as well as bronchial phlegm formation (h, H&E stain, 200×) are visible.

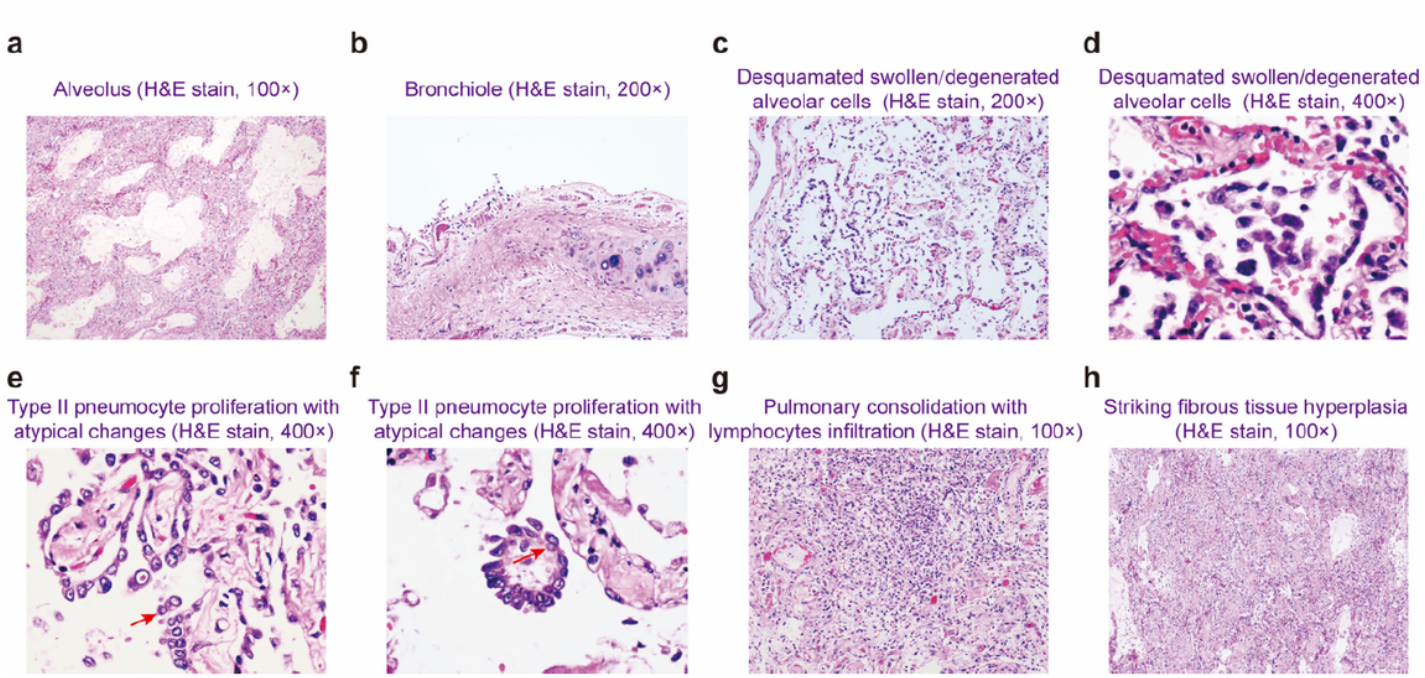

Figure 2

Damage of respiratory tracts and reparative changes. a-b, Intensive losing of alveolar (a, H&E stain, 100×) and bronchiole (b, H&E stain, 200×) epithelial cells. c-f, Desquamated swollen and degenerated alveolar cells in alveoli (H&E stain, c, 200× and d, 400×); type II pneumocyte proliferation with atypical changes (e and f, H&E stain, 400×): enlarged nuclei, clearing of nuclear chromatin and prominent nucleoli. Suspected viral inclusions are indicated by arrow. g-h, Pulmonary consolidation with infiltration of lymphocytes (g, H&E stain, 200×) and striking fibrous tissue hyperplasia (h, H&E stain, 100×).

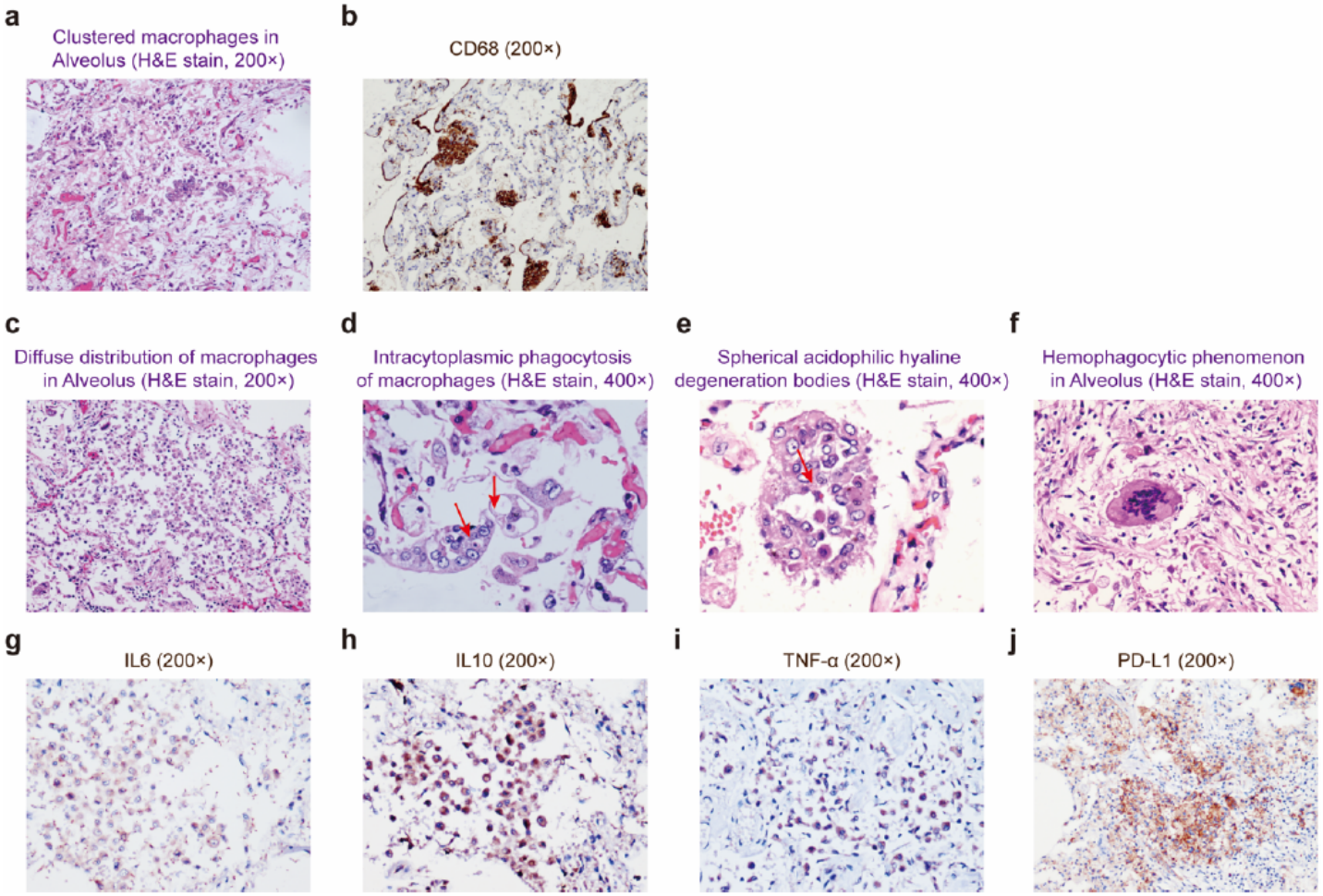

Figure 3

Aggregated alveolar macrophages. a-f, A large number of mononuclear and multinucleate macrophages in alveoli in varied forms: in clusters (a, H&E stain, 200×) and immunohistochemistry staining of CD68 (b); Diffuse distribution (c, H&E stain, 200×); Intracytoplasmic phagocytosis (d, H&E stain, 400×, indicated by red arrow) and Spherical acidophilic hyaline degeneration bodies (indicated by orange arrow); Hemophagocytic phenomenon (e, H&E stain, 400× indicated by red arrow) and multinucleated giant cell (f H&E stain, 400×). g-j, Expression of chemokine and inflammatory cytokines: IL-6, IL-10, TNFα (g-i, 200×) and extensive expression of PD-L1 (j, 200×)

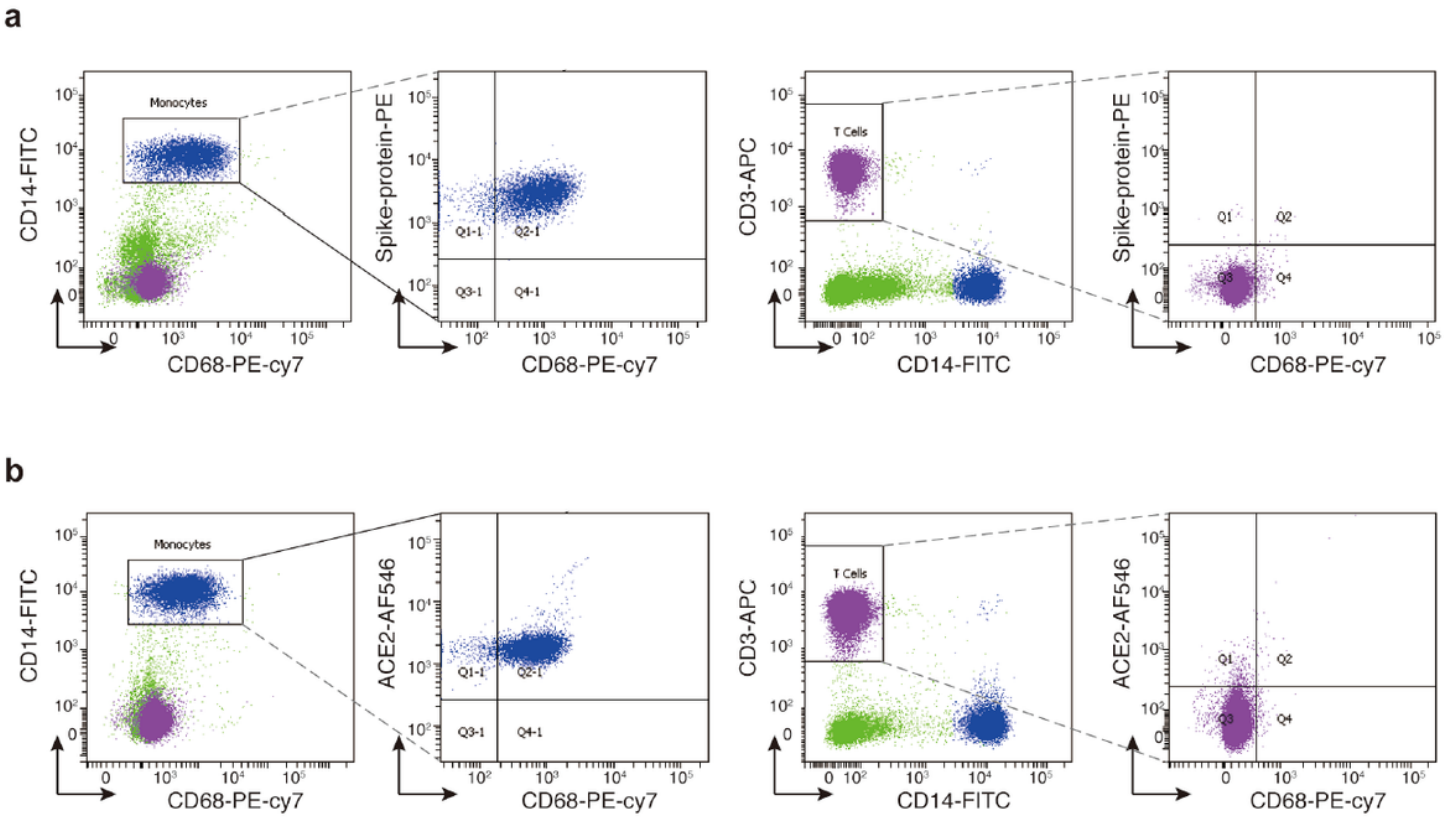

Figure 4

SARS-CoV-2 Spike protein interaction with CD68 macrophage. a, Flow cytometry analysis showing the distribution of S protein bound cells. CD14 markers were used for labelling myonocytes/macrophages while CD3 for T cells. b, Flow cytometry analysis showing the expression of ACE2 in T cells and monocytes/macrophages.

Supplementary Files

This is a list of supplementary files associated with this preprint. Click to download.

- SupplementaryFigures15.pdf
- SupplementaryTable1.docx